

# Experimental Assessment of the Active Flow Control over the Flight Deck of a Frigate

Elvina Derhille<sup>1†</sup>, Laurent Keirsbulck<sup>2</sup>, Quentin Gallas<sup>3</sup>, and Luc Bordier<sup>4</sup>

<sup>1</sup>ONERA - The French Aerospace Lab, 59014 Lille, France

<sup>2</sup>Department of Mechanical Engineering, LAMIH UMR8201, 59313 Valenciennes, France

<sup>3</sup>ONERA - The French Aerospace Lab, University of Toulouse, F-31410 Mazzac, France

<sup>4</sup>Hydrodynamic Modelling and Simulations, NAVAL GROUP/SIREHNA, 44340 Bouguenais, France

<sup>†</sup>Corresponding author: elvina.derhille@onera.fr

## Abstract

The airwake of a simplified ship model, representative of the geometry of a frigate at 1:50 scale, is studied experimentally in a wind tunnel. The shipboard landing operation requires a high workload from the pilots. The objective is to improve - in sense of pilot workload - the flow topology over the flight deck. For this purpose, active flow control is implemented. The slots are located along the sides of the hangar, three blowing speeds are studied and the orientation of the blowing is done with different angles. The analysis is based on stereo particle image velocimetry and pressure sensors. Results show a reduction of the recirculation area above the flight deck, observed at 0 and at 20 degrees yaw angle starboard too. Turbulent intensity increases in the recirculation bubble, not outside. At the landing point, the flow is no longer downward due to the control. Results show a small impact of the control in the presence of a rotor in a hover position over the flight deck.

## Nomenclature

$C_p = (P - P_0)/(1/2\rho U_\infty^2)$	Mean pressure coefficient [-]
$H$	Hangar height [m]
$L_r$	Reattachment length [m]
$Re_H = U_\infty H/\nu$	Reynolds number based on the height of the hangar [-]
$U_\infty$	Free stream velocity [m/s]
$U_j$	Mean velocity blowing [m/s]
$U, V, W$	Mean velocity component [m/s]
$x, y, z$	Spatial coordinates [m]
$X_r$	Spatial coordinate of the reattachment point [m]
$\alpha_s, \alpha_p$	Separated shear layer angle at starboard and at port [degree]
$\theta$	Angle of blowing [degree]
$\omega_z$	Spanwise mean vorticity [ $m/s^2$ ]
$\nu$	Kinematic viscosity of the air at ambient temperature [ $m^2/s$ ]
$\rho$	Density [ $kg/m^3$ ]

## 1. Introduction

When designing the frigate, one of the objectives was to design a stealthy surface ship. The inclination of its hull reduces its radar surface, but its sharp edges greatly degrade the ship's aerodynamics. The flight deck for helicopters is located at the aft. It is a restricted and highly turbulent space. The landing is complex and requiring a high workload. Helicopter landing operations on ship are challenging for the pilots due to the aerodynamic interaction of the helicopter wake with the flow perturbations caused by superstructure of the ship. The flow on the helideck is highly turbulent and pilots must go through strong airwake for landing operations. The addition of helidecks movements, rotor wake, visibility and pilot experience to this unsteady flow conditions is often characterized by an increased workload for the pilots.<sup>1</sup>

## ACTIVE FLOW CONTROL OVER A FRIGATE FLIGHT DECK

Because of the hangar sharp edges and the presence of superstructure on the frigate roof, an unsteady flow field appears above the flight deck. A shear layer is separated at the edge of the hangar and reattached downstream in the flight deck. Between these points there is a recirculation bubble with strong velocity gradients where the helicopters should land. The approach path to the ship requires to traverse the flight deck establishing a steady hover 5 m above the center of flight deck before descending vertically and landing.<sup>2</sup>

In addition to these constraints during the landing procedure, there is the difficulty of establishing - and even more so of predetermining - the operational limits. To date, only the Ship Helicopter Operating Limits (SHOL) allows to answer this question. It defines the boundaries of safe operation for a particular ship-helicopter combination in terms of maximum allowable wind speed and direction relative to ship. The development of SHOL requires to perform numerous trials at-sea that are extremely expensive, time-consuming and associated with high risk.<sup>1</sup> To alleviate these constraints, researchers have shown promising results with active flow control applied on the helideck<sup>3,4</sup>. However, there are no links yet made between aerodynamic characteristics and pilot workload. Control objectives are not known and defined because there is no pilot workload criterion. Therefore, the concepts developed and the impact they may have on a possible improvement of landing conditions are subject to further and more thorough validation.

This paper presents a study of the flow field over a frigate landing deck and the application of steady blowing for active flow control over a frigate model. Once the study of the base flow field is completed, the flow field was modified in the backward facing step using steady blowing. The paper is organised as follows: section 2 presents the experimental setup, section 3 defines the mean flow and the parameters used for further scaling, sections 4 and 5 present the experimental results without and with yaw angle, and section 6 is devoted to the quantification of the aerodynamic effect of a rotor in hovering position above the flight deck.

## 2. Experimental Configuration

### 2.1 Onera L2 Wind Tunnel and model geometry

The experiments are conducted in the L2 low-speed wind tunnel at Onera Lille. The test section is closed and rectangular (6 m width by 2.4 m height by 13 m long). A turntable setup of 5.96 m in diameter allows the azimuthal adjustment. Maximum speed can reach 19 m/s. In these experiments, the side slip angle varies from -40 to 40 degrees by 10 degrees step. The upstream velocity  $U_\infty$  is measured by pitot probe located at the test section inlet and is set to 15 m/s, equivalent to about 30 kn.

The ship model consists of a simplified but representative frigate geometry at the 1:50 scale. The Reynolds number based on the height of the hangar is defined as  $Re_H = U_\infty H / \nu$  where  $\nu$  is the kinematic viscosity of the air at ambient temperature. Most of the results are conducted with  $U_\infty = 15$  m/s, corresponding to  $Re_H = 1.3 \times 10^5$ . For reference, a Cartesian coordinate system is used with x the streamwise, y the spanwise direction and z the transverse or cross-stream. Its origin  $O$  is arbitrarily set on the deck platform at the middle of the rear end of the deck.

### 2.2 Measurements setup

#### Pressure Measurements

The helideck platform is equipped with 88 equally spaced static pressure taps, 32 additional static pressure taps are on the superstructure and the hangar door. Pressure measurements are presented in the non-dimensional  $C_p$  data, the reference pressure  $P_0$  is taken in the wind tunnel test section.

#### PIV Measurement

A specific setup is used for the SPIV measurements. The laser source and the mirror are directly integrated into the model and an optical glass replaces a part of the hangar door (Fig. 1). Two PIV configurations are used to measure the flow field above the flight deck, one parallel to the platform with the plane at mid-height of the hangar ( $z/H = 0.5$ ) and a perpendicular one with the plane oriented along the deck centreline ( $y/H = 0$ ). The two cameras used for the PIV measurements are located either on the wind tunnel roof or on the turning table on the floor for, respectively, the parallel or perpendicular configuration. By such embedded setup, the recording of the flowfield at different side slip angle is made easier. It consists in traversing a total pressure probe along each slot to measure the spatial homogeneity, and to calibrate the transfer function between the input pressure and the out massflow to reach the velocity ratio targets.

## ACTIVE FLOW CONTROL OVER A FRIGATE FLIGHT DECK

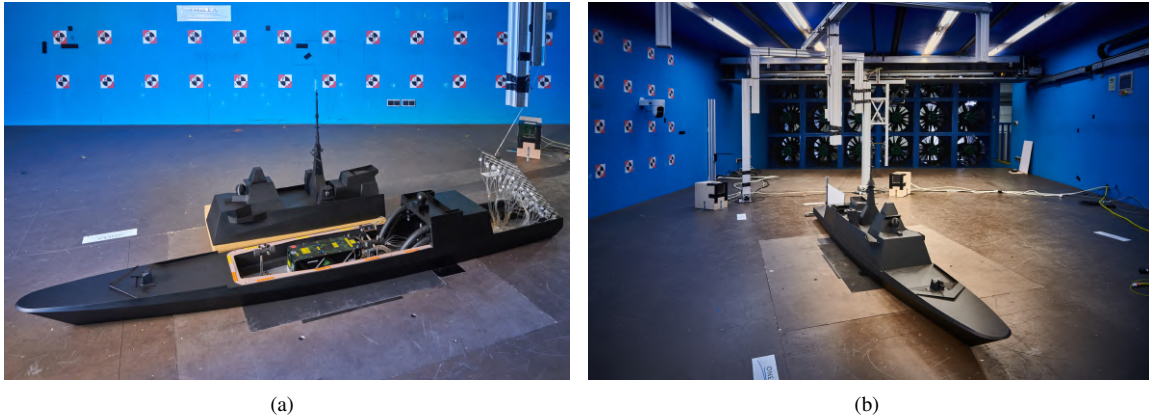


Figure 1: Representation of **a** the instrumentation of the model and the embedded SPIV system, and **b** S-PIV setup for the perpendicular configuration showing the calibration plane in L2 wind tunnel.

### 2.3 Steady Blowing Slots

The active flow control is realised by continuous blowing through eight slots of 2 mm width located along the sides of the hangar. The blowing jets exit tangentially to the geometry side toward the flight deck platform (angle of 0 deg) or with an angle of 30 deg toward the center flight deck platform. The incoming mass flow comes from underneath the wind tunnel and separates into four branches that independently feed four pair of slots. This power supply allows independent adjustment by pair of the eight slots. Here three velocity ratios ( $U_j/U_\infty$  equal to 2, 3 and 4) are used in the wind tunnel experiments, where  $U_j$  is the mean jet velocity at the slots exit. The characterisation was made earlier on the test bench presented on Fig. 2.

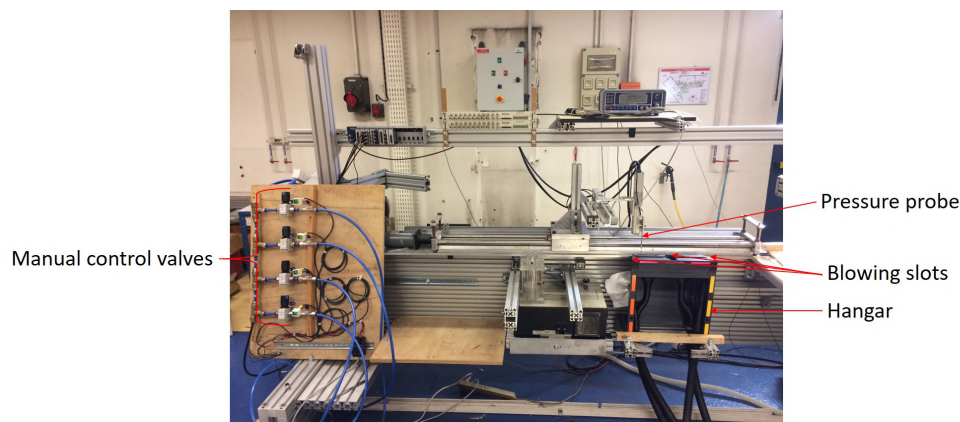


Figure 2: Test bench to characterise the blowing jets.

### 2.4 Rotor parameters

The change in direction and intensity of speeds due to the recirculation bubble is felt by the pilots. The rotor blades entering the deck absorb a flow with over velocities than the outgoing blades, which can lead to instabilities for the helicopter and therefore complex situations for the pilot during the procedure. Whatever the approach path, the last phases are common. The pilot is in a hover position before the descent phase to arrive at the landing position. Hovering has been identified like asking the most workload for the pilots.<sup>5</sup> The hover position (Fig. 3) is at  $x/H = -2$  in these test configurations. The model used in this experimental study is a 4-bladed rotor model. It has a diameter of 0.28 m and his aerodynamic performances are set to simulate the induce flow of a NH-90 helicopter.

## ACTIVE FLOW CONTROL OVER A FRIGATE FLIGHT DECK



Figure 3: Ship model on scale 1:50 with the rotor simulator in hover position before the descent phase installed in the L2 wind tunnel.

### 3. Baseline Flow Characteristics in Streamwise Direction

Before analysing the effects of blowing on the 3D backward facing step, we briefly review some aspects of its uncontrolled flow. Many research have been performed to study the flow field over a 2D backward facing step both experimentally and computationally<sup>6</sup>. It basically consists in an unsteady, separated shear layer with vortex structures, which emanates from the top of the hangar and it is reattached downstream. This phenomenon is highly turbulent. Under the shear layer a recirculation bubble zone appears. Inside this bubble there are high instabilities and large velocity gradients. Extending the problem into three dimensions it is observed the appearance of a lateral flow entering from the side of the ship. This lateral flow causes the flow field over the flight deck to be three-dimensional and the appearance of a horseshoe vortex structure that will not be stationary<sup>7</sup>.

The mean spanwise vorticity underlines the boundary layer separation at the edge of the hangar. The formed shear layer is detached from the hangar, increasing in width throughout the streamwise direction. The shear layer is globally represented in Fig. 5(a) as the negative vorticity region. Beneath the shear layer, a recirculation zone is observed. As the flow separated of the back edge off the hangar, high vorticity magnitude layers propagated downstream. The angle of the separated shear layer with the starboard and port edge of the hangar can be used as a comparative metric for the effect of control on the closure along  $y$  of the recirculation bubble.

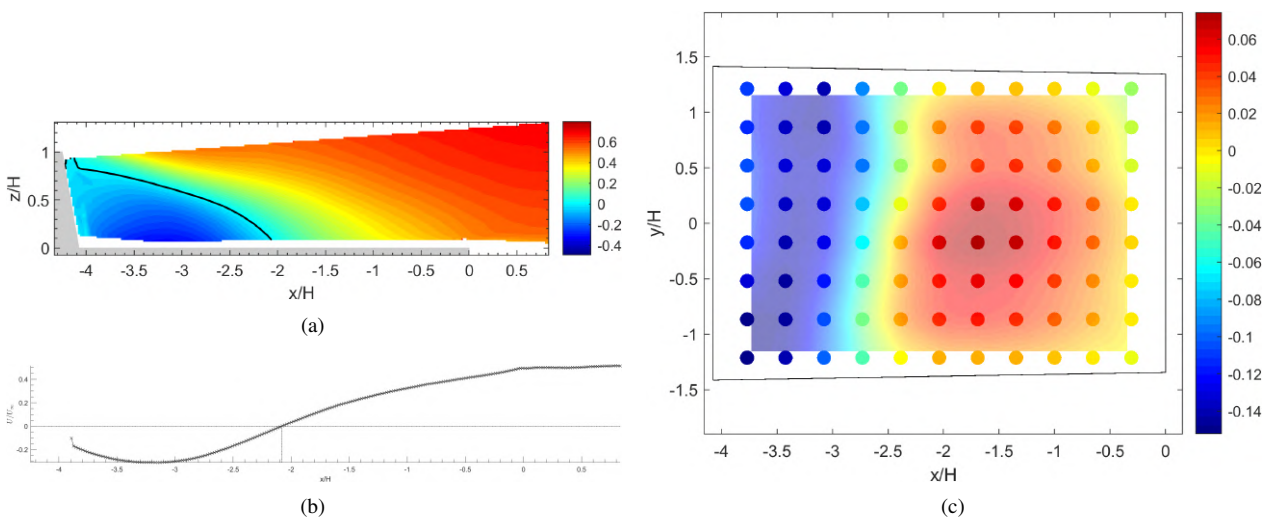


Figure 4: Non-dimensional mean properties of the baseline flow at  $Re_H = 1.3 \times 10^5$ . **a** Time-averages streamwise velocity  $U/U_\infty$  with the iso-value line  $U/U_\infty = 0$ . The reattachment point  $X_r$  is displayed by the vertical dashed line, **b** velocity profile extracted from (a) at  $z/H = 0.008$ , and **c** Mean base pressure coefficient on the deck surface.

Now, the properties of the recirculation region are presented. The time-averaged velocity components and base pressure distribution on the deck are presented in Fig. 4 at  $Re_H = 1.3 \times 10^5$ . The negative values of  $U$  in Fig. 4(a) indicate the existence of a recirculation field. The length of the recirculation zone and the spatial coordinate of the

reattachment point are noted, respectively,  $L_r$  and  $X_r$ .

The mean wake is dominated by a large clockwise recirculating motion over the half of the deck platform. This is visible when analysing the base pressure distribution on the deck surface (Fig. 4(c)), a low pressure zone is established and it is associated with the large clockwise recirculating motion which curves the streamlines generating high pressure gradients and a local pressure drop.

#### 4. Flow Control Results

The objectives of control are unknown, in terms of pilot workload alleviation. The intention is to develop flow control devices to mitigate or eliminate the effects of upstream geometrical elements - superstructure, sharp edges, vertical wall near the landing point - that generate a disturbed flow field strongly affecting the pilot. However, there is no link yet between parameters used to describe the flow and the pilot workload level. Therefore, the concepts developed in this section and the impact they may have on a possible improvement of landing conditions are subject to further and more thorough validation.

The mean flow is presented at zero degree yaw angle without and with control. For the uncontrolled case, it is composed of the classical features that are found in the literature.<sup>4</sup> At the hangar top and sides, the incoming flow separates from the geometry to form a recirculation bubble standing above the helideck and closing the middle of the platform. The recirculation region is composed of two counter-rotating vortices in the parallel plane and a large one in the vertical plane, similar to the academic 3D backward facing step flow topology. Then, Fig. 5(b) shows the effect of steady blowing applied on the eight slots around the hangar, with a velocity ratio  $U_j/U_\infty = 3$ . The recirculation bubble decreases in size and the shear layer is bent inward. Outside the recirculation bubble, without control the streamlines are deviated towards the flight deck, and with blowing the streamlines are straightened and parallel to the flight deck. The pilot would carry out the descent phase with a flow of intensity close to the upstream infinite speed and whose direction is mainly along the streamwise  $x$  direction.

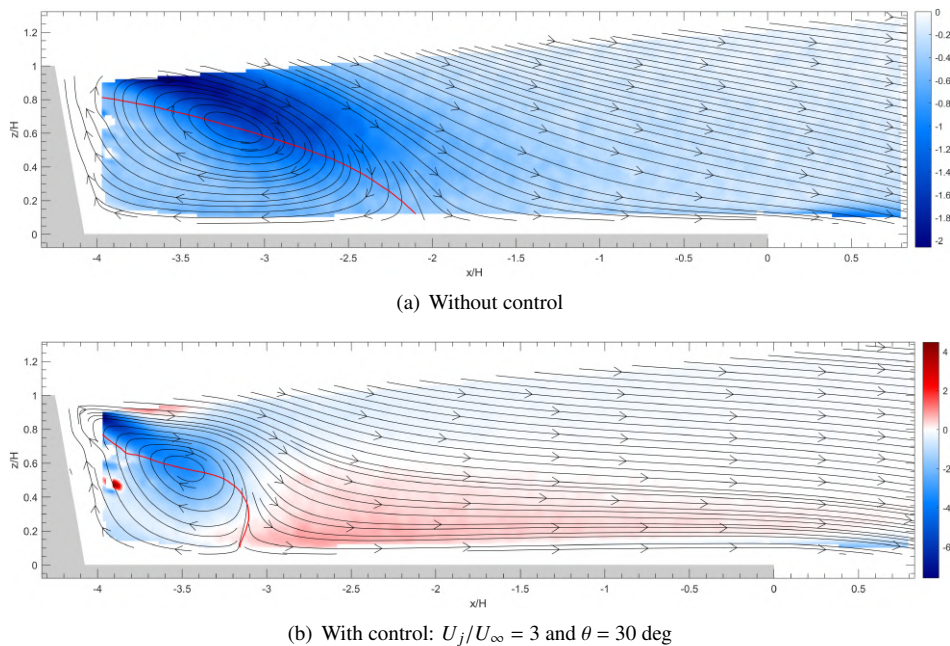


Figure 5: Non-dimensional, mean vorticity  $\omega_z \cdot H/U_\infty$  and associates streamlines. The red line denotes the zero streamwise velocity value. Perpendicular plane  $y/H = 0$  at zero degree yaw angle.

Figure 8 compares the mean profiles in the spanwise direction without and with blowing. Inside the recirculation zone (Fig. 8(a)) blowing forces the recirculation bubble to contract along  $y$ , the velocity along  $x$  slightly increases and the vertical velocity greatly increases. At the landing point (Fig. 8(b)) the variation of streamwise velocity is low contrary to the vertical one. At the landing point there is an upward flow.

Figures 9 and 10 show in more detail the control effect in the horizontal and vertical planes, respectively. Results with the blowing at  $U_j/U_\infty = 3$  are presented. The blowing effect decreases the recirculation bubble size by shortening it in both the streamwise and spanwise directions. On the recirculation boundaries, the shear layer makes a higher angle

## ACTIVE FLOW CONTROL OVER A FRIGATE FLIGHT DECK

with the streamwise direction (Table 2), angles are measured in degrees inboard from the flight deck and all values are positive.

Table 2: Separated shear layer angle. With control for  $\theta = 30$  deg blowing

Ratio jet $U_j/U_\infty$	0	1	2	3
$\alpha_s$ [deg]	6.1	31.1	43.8	50.6
$\alpha_p$ [deg]	6.1	25.1	40.0	44.1

The correlations of the three fluctuating velocity components, namely  $\langle u'u' \rangle$ ,  $\langle v'v' \rangle$ , and  $\langle w'w' \rangle$  and the turbulent kinetic energy  $K = 1/2(\langle u'u' \rangle + \langle v'v' \rangle + \langle w'w' \rangle)$  are in Fig. 9 and 10. The turbulent intensity is the same in the wake. For the uncontrolled case the turbulent intensity is low in the recirculation zone, while with blowing the turbulent intensity increases in the recirculation bubble. In more detail, some regions of the flow can be associated with a specific component: i) the largest contribution of longitudinal fluctuations is at the top of the shear layer, ii) in the centre of the recirculation bubble are the up and down fluctuations and iii) near the deck is the transverse component. On the one hand, the turbulent intensity in the area of interest is therefore not changed overall by the control. On the other hand, it greatly modifies the average flow.

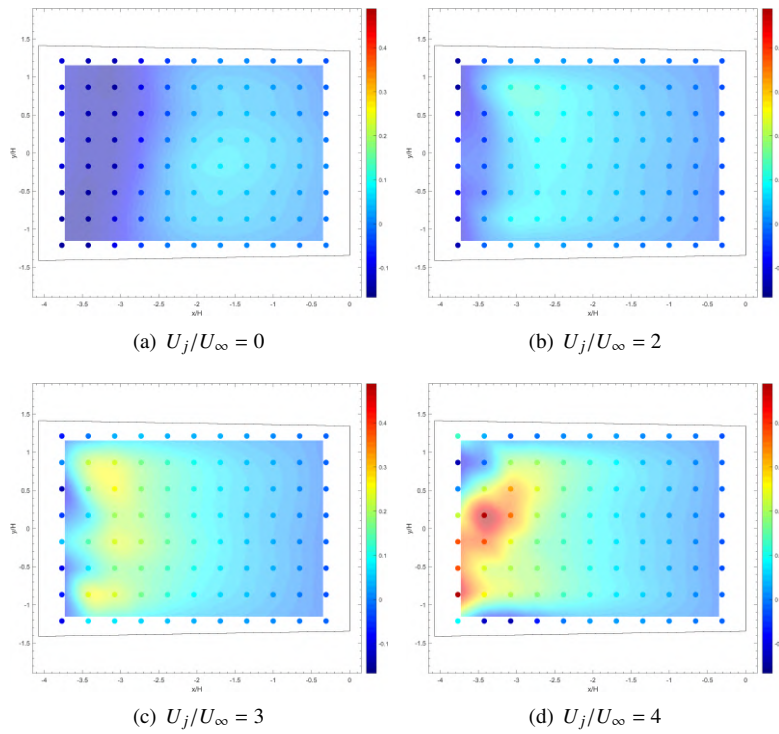
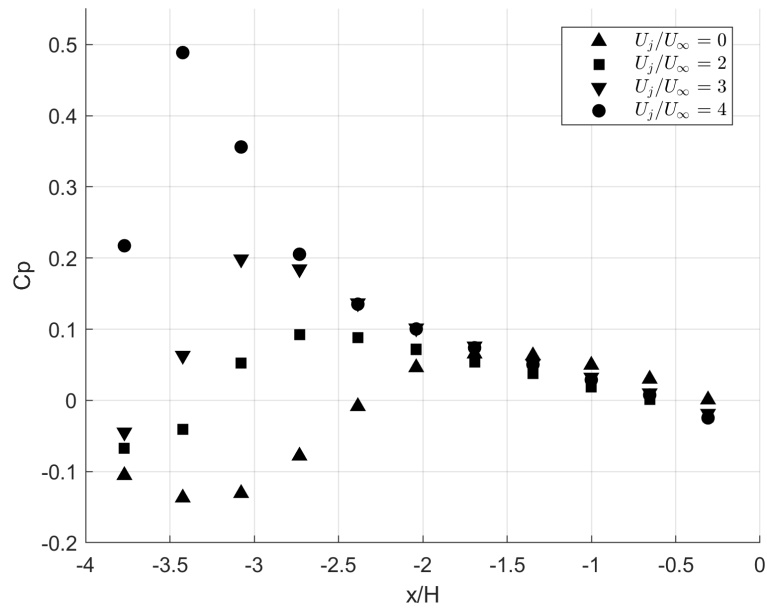
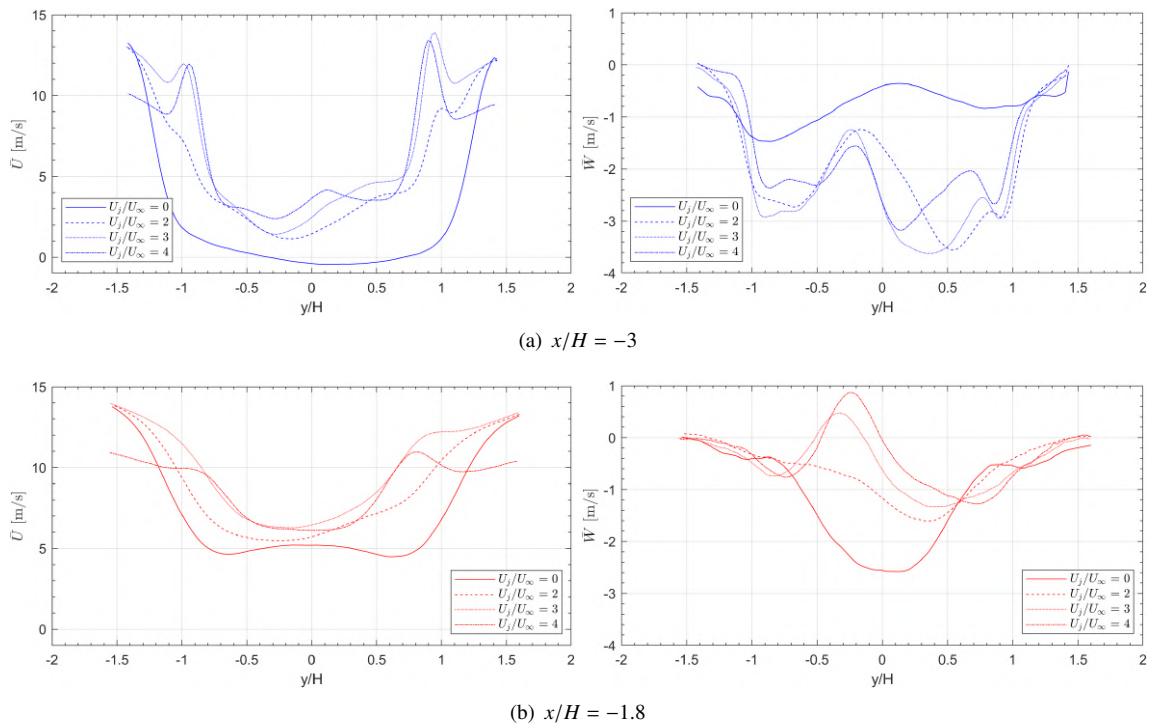


Figure 6: Mean pressure coefficient at the platform surface at zero degree yaw angle, without and with control.

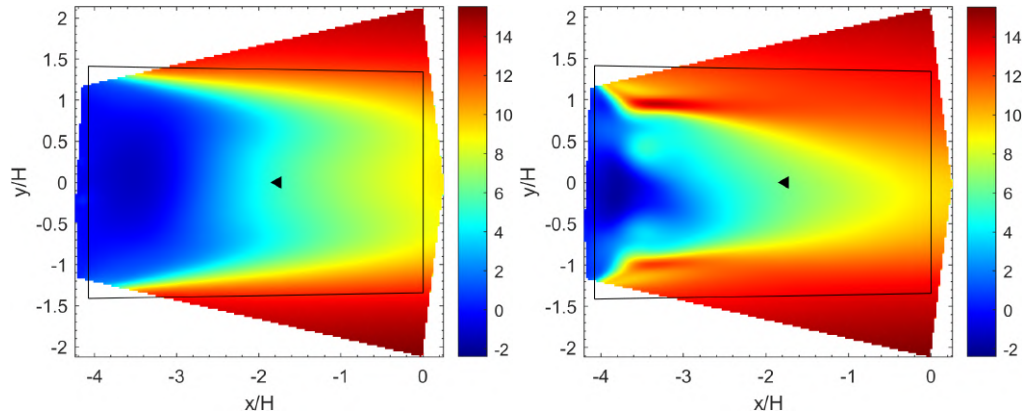
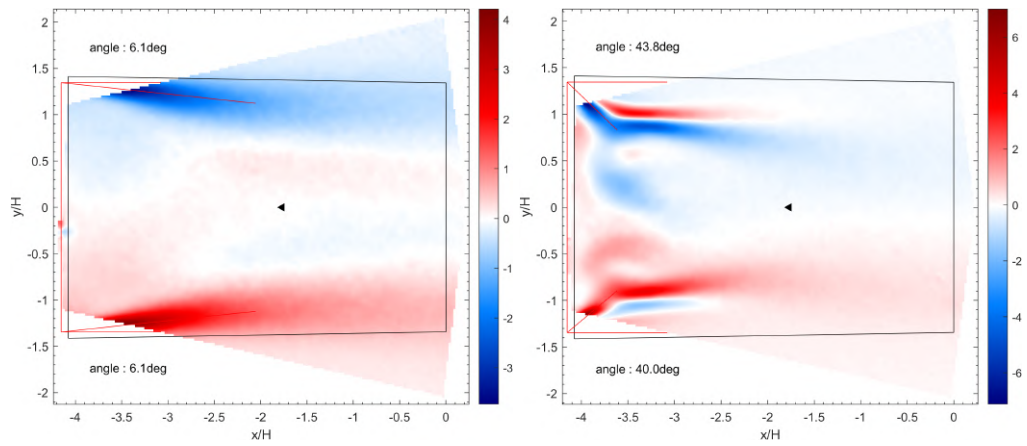
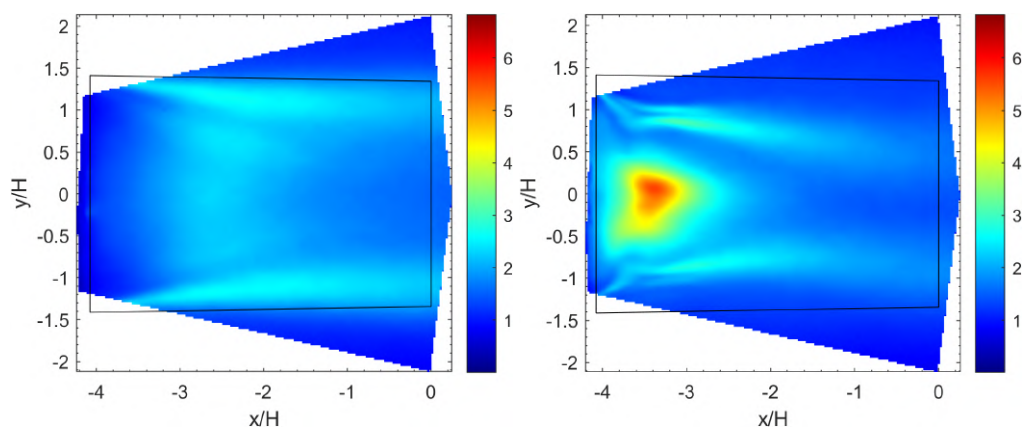
The analysis from velocity measurements by S-PIV are confirmed by the pressure measurements on the deck (Fig. 6). The same spatial coordinates of the attachment point are identified from the mean pressure coefficients, an increase of the blowing speed induces a reduction of  $X_r$ . It is interesting to note that blowing does not affect the pressure profile along  $y/H = 0$  beyond  $X_r = -2$ , which corresponds to the attachment point of the uncontrolled case (Fig. 7s confirmed with the distribution across the entire deck (Fig. 4(c)). The recirculation footprint is reduced due to the blowing.

In conclusion, the recirculation region is reduced with blowing toward the centre of the deck. The turbulence activity is increased inside this region and the same outside. Conversely, the averaged values are significantly modified outside the recirculation zone. In the wake, the flow is no longer downward but close to the upstream infinite flow, i.e. it is homogeneous and mainly in the streamwise direction.

## ACTIVE FLOW CONTROL OVER A FRIGATE FLIGHT DECK

Figure 7: Mean pressure coefficients without and with blowing at  $y/H = 0$ .Figure 8: Profiles of mean velocity  $U$  and  $W$ , without and with blowing, **a** inside the recirculation region and **b** at the landing position. Horizontal plane  $z/H = 0.5$ .

## ACTIVE FLOW CONTROL OVER A FRIGATE FLIGHT DECK

(a)  $U$  (m/s)(b)  $\omega_z \cdot H/U_\infty$ (c)  $\langle u'u' \rangle$  ( $m^2/s^2$ )

## ACTIVE FLOW CONTROL OVER A FRIGATE FLIGHT DECK

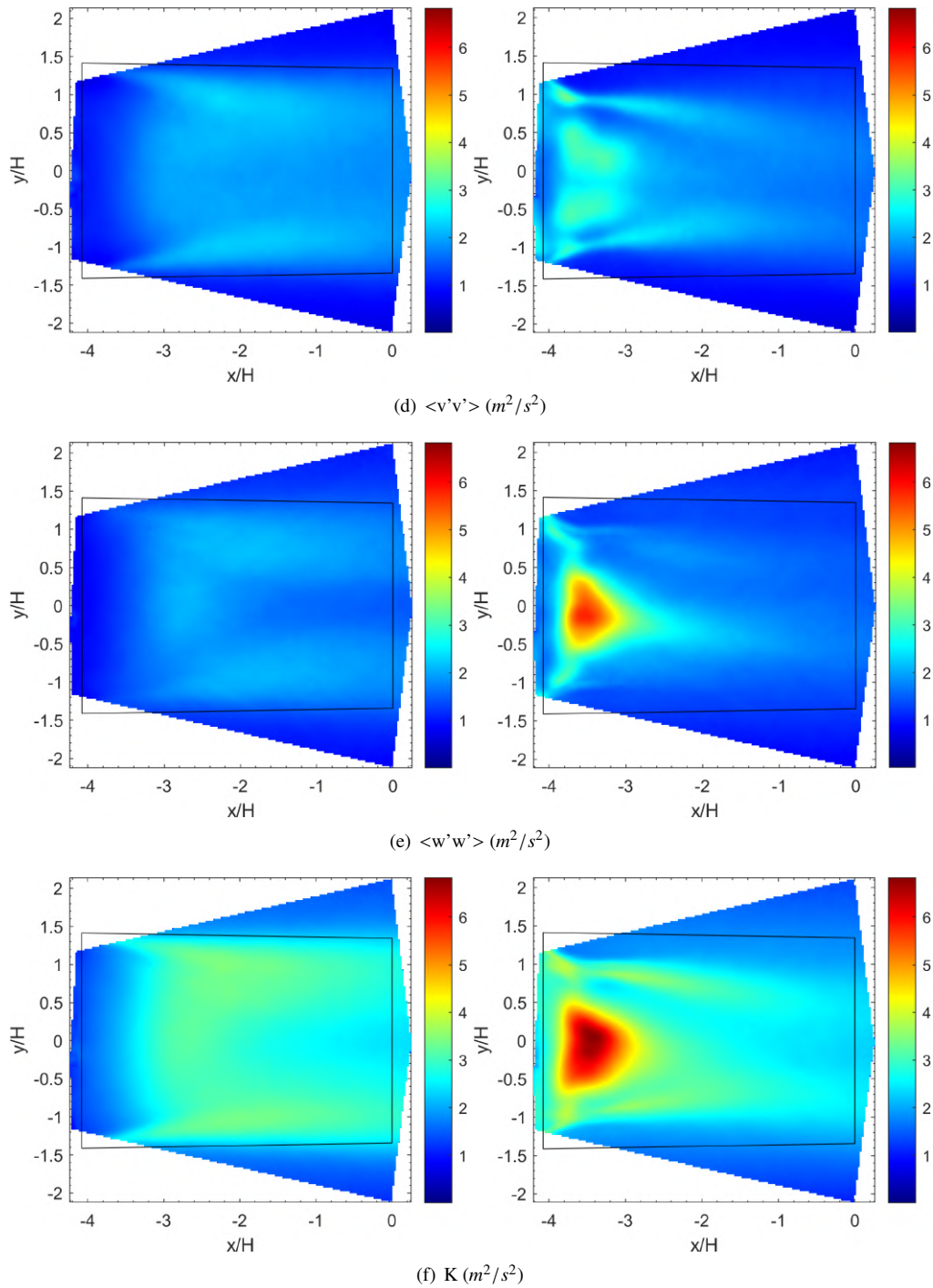


Figure 9: Velocity field comparison without and with blowing ( $U_j/U_\infty = 3$ ) at zero yaw angle. Horizontal plane  $z/H = 0.5$ . **a**  $U$  [m/s], **b**  $\omega_z \cdot H/U_\infty$ , **c**  $\langle u'u' \rangle$  [ $m^2/s^2$ ], **d**  $\langle v'v' \rangle$  [ $m^2/s^2$ ], **e**  $\langle w'w' \rangle$  [ $m^2/s^2$ ], **f**  $K$  [ $m^2/s^2$ ].

## ACTIVE FLOW CONTROL OVER A FRIGATE FLIGHT DECK

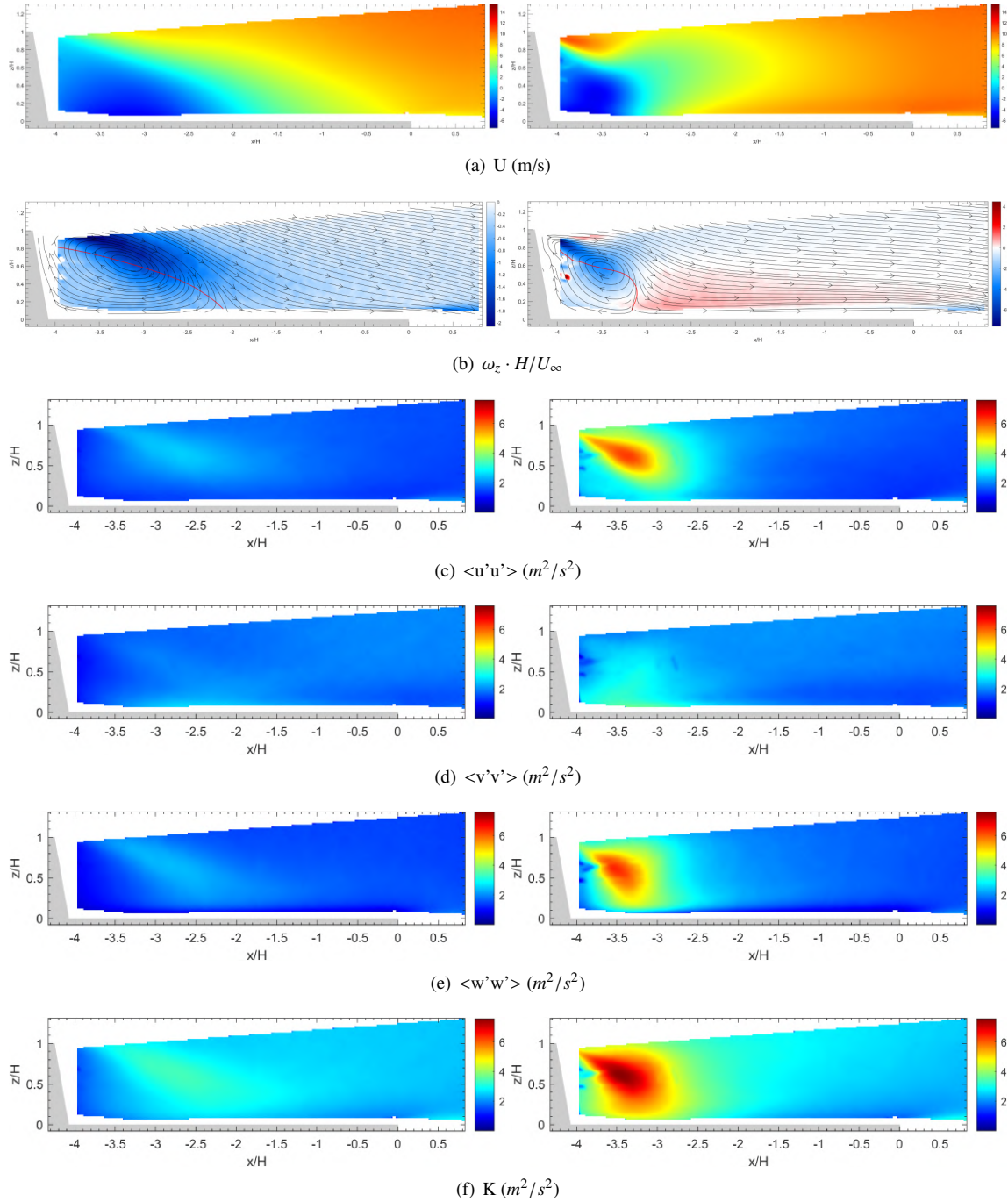


Figure 10: Velocity field comparison without and with blowing ( $U_j/U_\infty = 3$ ) at zero yaw angle. Vertical plane  $y/H = 0$ . **a**  $U$  [m/s], **b**  $\omega_z \cdot H/U_\infty$ , **c**  $\langle u'u' \rangle$  [ $m^2/s^2$ ], **d**  $\langle v'v' \rangle$  [ $m^2/s^2$ ], **e**  $\langle w'w' \rangle$  [ $m^2/s^2$ ], **f**  $K$  [ $m^2/s^2$ ].

## 5. Flow Control Results with yaw angle

The ship model is rotated in the L2 wind tunnel by 10 deg steps. An analysis similar to the one performed for the 0 deg yaw angle configuration can be made. Figure 11 presents the blowing effect for the 20 degree yaw angle starboard on the pressure distribution on the deck. Different configurations of blowing are performed: i) all the slots are blowing, ii) only those on the starboard side (blue slots on Fig.11(a)) and iii) those on the port side (orange slots on Fig.11(a)). Blowing on the other side of the wind promotes the expansion of the recirculation zone. Conversely, blowing on the windward side will re-symmetrise the pressure footprint on the flight deck.

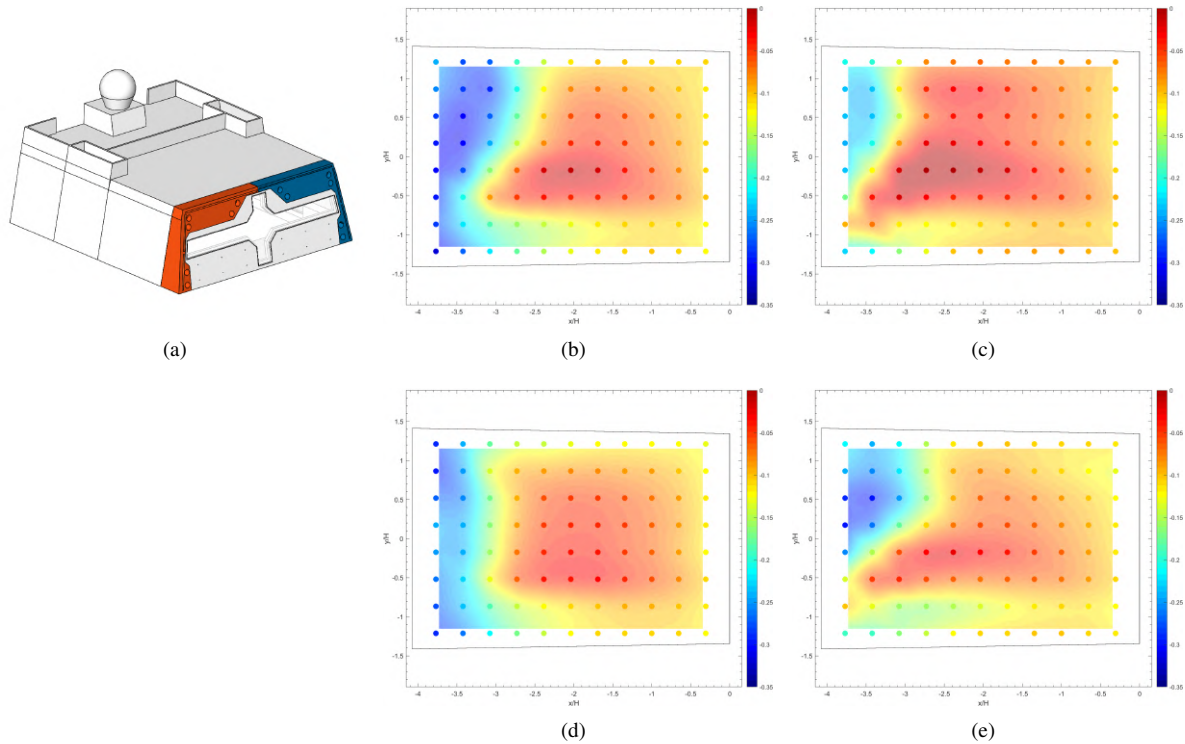


Figure 11: **a** CAD of the hangar element. Mean pressure coefficient at the platform surface at 20 degree yaw angle starboard, **b** without control, with control at  $U_j/U_\infty = 2$  and different blowing configurations: **c** all slots are blowing, **d** only those on the starboard side, **e** those on the port side.

Figure 12 shows the module velocity field in the horizontal plane for both the uncontrolled and controlled case ( $U_j/U_\infty = 3$ ). It shows a similar behaviour to the pressure distribution. The recirculation bubble is asymmetric and extends more to the windward side. Blowing does not correct this asymmetry but acts on the expansion along  $x$ . As in the case of zero yaw angle, the control reduces the recirculation area. These results demonstrate the ability of the blowing system to control and deviate the flow behaviour with yaw angle.

To conclude this section, the application of constant blowing is shown to be effective in decreasing the recirculation zone above the deck for yaw angles equal to 20 degree. Asymmetric blowing may be more efficient according to the wind direction. The possible improvement when landing with a crosswind is subject to further and more thorough validation. Furthermore, the effects of all these changes made by the control should be: first be felt by the pilot and then be characterised as an improvement or not. However, only the flow of the frigate was studied here and presented in this paper. The intrusion of the rotor into the wake impacts this flow, the recirculation bubble detaches from the hangar and is accelerated,<sup>8</sup> as shown in the next section.

## ACTIVE FLOW CONTROL OVER A FRIGATE FLIGHT DECK

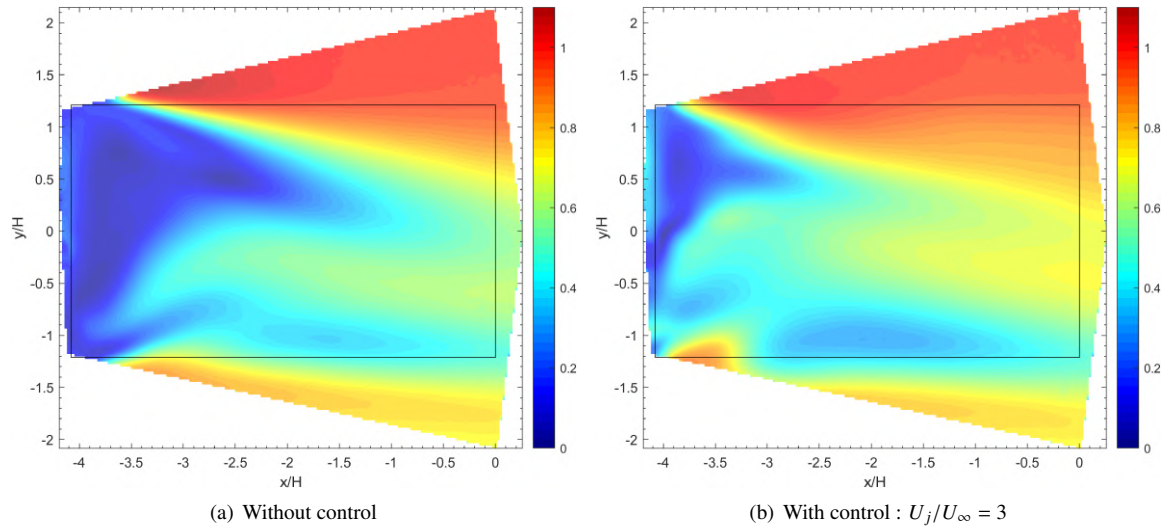


Figure 12: Module of velocity without and with blowing ( $U_j/U_\infty = 3$ ) at 20 yaw angle starboard. Horizontal plane  $z/H = 0.5$ .

## 6. Helicopter/Ship Interaction

The last phase of the test campaign was devoted to the quantification of the aerodynamic effect of the rotor in hovering position above the flight deck. With the experimental setup explained in section 2, the velocity maps in the longitudinal plane obtained by S-PIV are presented in Fig. 13.

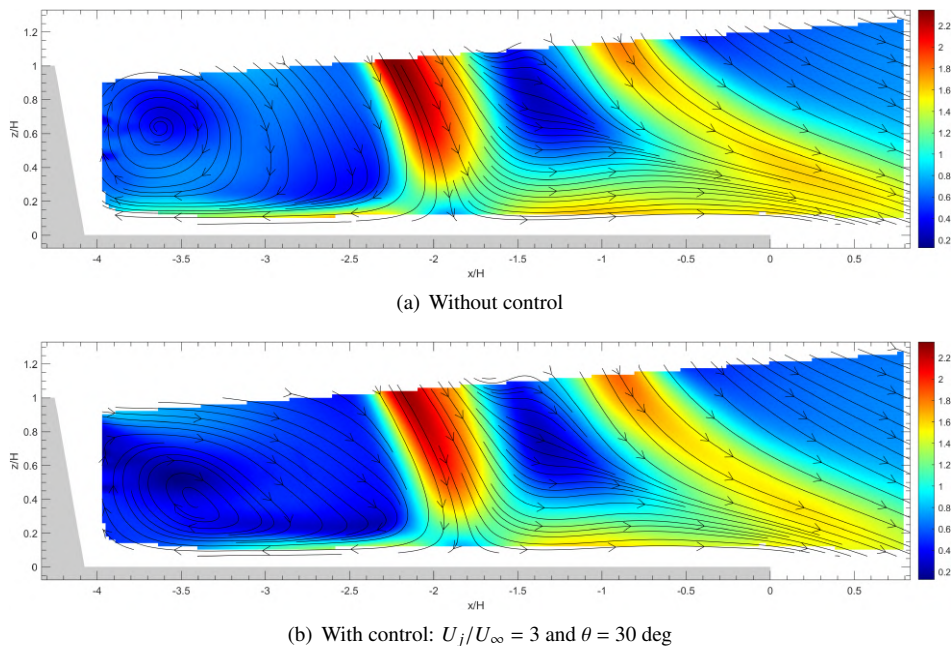


Figure 13: Module of velocity obtained with the rotor in hover position, without and with blowing ( $U_j/U_\infty = 3$ ) at 0 yaw angle. Vertical plane  $y/H = 0$ .

In that position, the rotor is partially affected by the low-velocity recirculation area generated over the flight deck. The half part of the rotor absorbs flow with less velocity than the other half. The upstream infinite flow is deflected downwards after the detachment at the hangar edge. The blast induced by the advancing rotor blade favours this downward flow. There is a velocity asymmetry in the jets. This asymmetry can lead to complex situations for the pilot. The jet from the forward blades hits the deck surface and is deflected partly downstream but also upstream. This upstream contribution feeds the recirculation bubble which is always present and accelerated.

The flow is essentially the same with the  $U_j/U_\infty = 3$  blowing towards the inside of the deck. However, it can be noted that the recirculation bubble is crushed and slightly less accelerated. The velocity of the back jet is marginally higher than in the uncontrolled case even though the asymmetry between the jets is still present. It should be pointed out that the impact of the helicopter fuselage is not taken into account in the experimental campaign.

## 7. Conclusion

In this paper, the flow over the flight deck of a representative frigate model has been studied on wind tunnels tests with S-PIV and measurements of the pressure on the deck platform. Active flow control was implemented through eight 2 mm thick slots located around the edges of the hangar. The steady blown air exits at an angle of 30 degrees towards the centre of the deck. Two S-PIV planes are made at the deck and the interaction with a rotor is studied. The purpose of these experimental measurements is to describe the controlled flow compared to the uncontrolled case. Based on these results the following conclusions can be drawn.

1. The recirculation region is reduced with blowing toward the centre of the deck. An increase of the blowing speed induces a reduction of recirculation length  $X_r$ . The turbulence activity is increased inside this region and the same outside. Conversely, the averaged values are significantly modified outside the recirculation zone. In the wake, the flow is no longer downward but close to the upstream infinite flow, i.e. it is homogeneous and mainly in the streamwise direction.
2. From the mean profiles in the spanwise direction without and with blowing: inside the recirculation zone blowing forces the recirculation bubble to contract along y, the velocity along x slightly increases and the vertical velocity greatly increases.
3. In addition, blowing effect is still present with yaw angle. The asymmetry of the flow due to the wind coming from the starboard side is amplified with a blowing applied only with half of the port side slots. However, blowing through the same side slots - i.e. starboard - re-symmetries the flow, opening a wide range of flow control strategies.
4. The interaction between the wake of the frigate and that of a rotor involves an asymmetry of the rotor jets. The upstream jet feeds the recirculation bubble which is accelerated. The impact of the control in the presence of the rotor is not very pronounced in the longitudinal plane. It may be noted, however, that the recirculation bubble is crushed and slightly less accelerated.

In conclusion, these results are encouraging for the issue of pilot workload reduction. With active control oriented towards the centre of the deck, the area covered by the recirculation bubble is reduced, the turbulent intensity near the landing point is minimally impacted, and the flow is no longer downward at the landing point. It can be assumed that these modifications are beneficial to the pilots. The link with the pilots' feelings has yet to be defined and is subject of ongoing work.

## Acknowledgements

This work is funded by ONERA and NAVAL GRROUP via a PhD scholarship. Their support is gratefully acknowledged.

## References

- [1] Modeling and simulation of the effects of ship design on helicopter launch and recovery. Technical report, OTAN, 2016.
- [2] G.D. Carico, R Fang, and all. Helicopter/ship qualification techniques. Technical report, OTAN, 2003.
- [3] Investigation of airwake control for safer shipboard aircraft operations. Technical report, OTAN, 2007.
- [4] Q Gallas, M Lamoureux, J-C Monnier, A Gilliot, C Verbeke, and J Delva. Experimental flow control on a simplified ship helideck. *AIAA Journal*, 55(10):3356–3370, 2017.
- [5] José Marcio Pereira Figueira. *The use of offline simulation tools to estimate Ship-Helicopter Operating Limitations*. PhD thesis, Université d'Aix-Marseille, 2017.

## ACTIVE FLOW CONTROL OVER A FRIGATE FLIGHT DECK

- [6] Pankaj M Nadge and RN Govardhan. High reynolds number flow over a backward-facing step: structure of the mean separation bubble. *Experiments in fluids*, 55(1):1–22, 2014.
- [7] Benjamin Herry. *Etude aérodynamique d'une double marche descendante 3D appliquée à la sécurisation de l'appontage des hélicoptères sur les frégates*. PhD thesis, Université de Valenciennes et du Hainaut Cambrésis, 2010.
- [8] Rafael Bardera, Juan Carlos Matias-Garcia, and Adelaida Garcia-Magariño. Piv helicopter rotor-ground and rotor-frigate interaction study. In *AIAA AVIATION 2020 FORUM*, page 2740, 2020.